scientific data

Check for updates

OPEN

DATA DESCRIPTOR

Individual Brain Charting: fifth release of high-resolution fMRI data for cognitive mapping

Ana Fernanda Ponce[1,19]✉, Himanshu Aggarwal[1,19], Swetha Shankar[1], Juan Jesús Torre[1], Ana Luísa Pinho[1,2,3], Alexis Thual[1], Chantal Ginisty[4], Yann Lecomte[4], Valérie Berland[4], Lucile Beriot[4], Laurence Laurier[4], Véronique Joly-Testault[4], Gaëlle Médiouni-Cloarec[4], Lucie Hertz-Pannier[4], Christine Doublé[4], Bernadette Martins[4], Marie Amalric[5], Stanislas Dehaene[5,6], Nadine Diersch[7], Thomas Wolbers[7], Meredith A. Shafto[8], John P. O'Doherty[9], Vincent Man[9], Raymond J. Dolan[10], Russell A. Poldrack[11], Anthony Stigliani[11], Kalanit Grill-Spector[11,12], Danielle Douglas[13], Andy C. H. Lee[13], David B. Keator[14], Steven G. Potkin[14], Dorita H. F. Chang[15], Nikolaus F. Troje[16], Bo-Cheng Kuo[17,18], Duncan E. Astle[17] & Bertrand Thirion[1]

The *Individual Brain Charting* project focuses on collecting functional Magnetic Resonance Imaging data across a large set of cognitive tasks from a fixed cohort of participants, within a standardized environment. This approach seeks to obtain refined cognitive phenotyping of individual brains, uncovering details of their functional organization. We present an extension to the dataset, integrating data from eleven participants obtained at 3T, from a fixed environment to minimize inter-site and inter-subject variability. This release further enriches the cumulative coverage of psychological domains, while introducing new concepts. It includes tasks on mathematical processing, spatial navigation, emotion recognition and memory, proactive control, oddball detection, reward processing, reaction time, biological motion perception, gambling, scene processing and working memory. In total, 18 tasks with 180 contrasts were added, and 54 cognitive components were included in the description of the ensuing contrasts. As the dataset becomes larger, the collection of the corresponding topographies becomes more comprehensive, leading to enhanced brain-atlasing frameworks. Aligned with open-access and data-sharing standards, this dataset emphasizes transparency and collaborative research.

[1]Université Paris-Saclay, Inria, CEA, Palaiseau, 91120, France. [2]Department of Computer Science, Western University, London, Ontario, N6A 5B7, Canada. [3]Brain and Mind Institute, Western University, London, Ontario, N6A 3K7, Canada. [4]CEA Saclay/DRF/IFJ/NeuroSpin/UNIACT, Gif-sur-Yvette, 91191, France. [5]Cognitive Neuroimaging Unit, INSERM, CEA, Université Paris-Saclay, NeuroSpin center, 91191, Gif-sur-Yvette, France. [6]Collège de France, Paris, 75005, France. [7]Aging, Cognition & Technology Group, German Center for Neurodegenerative Diseases (DZNE), Magdeburg, 39120, Germany. [8]Department of Psychology, University of Cambridge, Cambridge, CB2 3EB, UK. [9]Division of the Humanities and Social Sciences, California Institute of Technology, Pasadena, California, 91125, USA. [10]Wellcome Centre for Human Neuroimaging, University College London, London, WC1N 3BG, UK. [11]Department of Psychology, Stanford University, Stanford, California, 94305, USA. [12]Stanford Neurosciences Institute, Stanford University, Stanford, California, 94305, USA. [13]Psychology (Scarborough), University of Toronto, Toronto, Ontario, M1C 1A4, Canada. [14]Department of Psychiatry and Human Behavior, University of California, Irvine, California, 92697, USA. [15]Department of Psychology, The University of Hong Kong, Stanford, Hong Kong. [16]Department of Biology, Centre for Vision Research, 4700 Keele Street, Toronto, ON, M3J 1P3, Canada. [17]Cognition and Brain Sciences Unit, Cambridge, CB2 7EF, UK. [18]Department of Psychology, National Taiwan University, Taipei, 10617, Taiwan. [19]These authors contributed equally: Ana Fernanda Ponce, Himanshu Aggarwal. ✉e-mail: ana.ponce-martinez@inria.fr

Background & Summary

Advancements in neuroimaging, particularly in *functional Magnetic Resonance Imaging* (fMRI), have greatly enhanced research on the human brain. fMRI allows researchers to map brain regions to functional domains, providing insights into the anatomical structures underlying human cognition. However, our understanding of all contributing factors, particularly of those related to individual variability and their implications in brain activity and behavioral differences, is still evolving[1–7]. To overcome this, there is a need for fMRI data that captures a wide range of activity patterns within individual brains. This involves exploring different cognitive domains, testing a variety of stimuli and conditions, all collected under consistent experimental parameters[1,7–10]. Such datasets make it possible to explore a broad range of brain responses, and open the way to comprehensive mappings and models of brain organization.

Motivated by this, the *Individual Brain Charting* (IBC) project began in 2014 with the goal of extensively collecting standardized fMRI data from a fixed participant cohort across diverse cognitive tasks to finely characterize individual topographies of cognitive components[11,12]. We present the latest release, extending the 1.5mm-resolution task-fMRI dataset for eleven participants to complete up to 40 hours of fMRI data per participant, with a target of 50 hours in the final release. The initial cohort comprised twelve participants, but after some participants dropped out, acquisitions described here include data from between eight and eleven subjects.

On every release, we focus on a different set of tasks. The first release[11] included protocols focused on perception, calculations and social reasoning[13–16]. The second[12] focused on higher-level functions, like mental time travel, theory-of-mind, and self-reference effect[17–23]. The third[24] featured movie-watching and retinotopic paradigms[25–27]. The fourth included various localizers and tasks involving discount processing and conflict detection[28–34]. The present edition marks the fifth release of the IBC dataset, and includes tasks on mathematics, spatial navigation, emotion recognition, action inhibition, gambling, reward processing, oddball detection, motor planning and motor control[35–43]. Table 5 shows the tasks' distribution across releases.

Along with data collection, we perform statistical analysis for every task. Up to this release, the dataset includes 67 tasks, comprising 530 contrasts described on the basis of 188 cognitive concepts extracted from the *Cognitive Atlas*[44]. We have introduced contrasts that delve into previously unexplored cognitive components such as geometric processing, gender perception, imagination, loss aversion, and motion coherence. The tasks probed in this release also included previously used concepts, such as combinatorial semantics or emotional expression, providing another opportunity to map their correlates. Figure 1 contains a workflow overview.

When selecting tasks for this release, we sought input from the research community and evaluated studies as they appeared in the literature. We contacted laboratories whose work targeted either cognitive domains not represented in earlier releases or domains already covered but investigated using different methodologies, stimuli, or experimental designs. These teams generously shared their protocols with us. By collecting all tasks under uniform conditions, IBC minimizes inter-site variability, and probing multiple conditions within the same brain creates a unique resource for comprehensive cognitive mapping. This approach serves as a strong foundation for developing brain function atlases and models.

The IBC project aligns with several initiatives that characterize individual brains while filling gaps by existing datasets. Notable examples include the *Midnight Scan Club*[45], the *Bold5000 Project*[46], the *Natural Scenes Dataset*[47], and the *Courtois-Neuromod* project[48], all of which collect extensive data from a small number of participants. Some of them include task-based fMRI acquisitions from various cognitive domains, and others focus on naturalistic stimuli. The IBC dataset complements these efforts and offers a broader range of cognitive domains and experimental paradigms, thereby extending individual-level mapping and advancing deep-phenotyping approaches in neuroimaging.

The IBC dataset is an open-access facility. Raw data and their derivatives are available in neuroimaging repositories, along with the different paradigms' material and scripts for analysis. Here, we give an account – focused on the present release– of the included tasks and experimental procedures.

Methods

To avoid ambiguity with MRI-related terms, definitions of these terms follow the *Brain-Imaging-Data-Structure (BIDS)* Specification (v1.9.0)[49]. Concretely, we adopt BIDS conventions for general entities such as *Modality, Data Type, Subject, Session, Run, Task*, and *Event*, as well as for modality-specific descriptors, including *Trial Type, Onset, Duration*, and all common MRI metadata fields. Throughout, the terms *subject* and *participant* are used interchangeably.

Participants. The present release of the IBC dataset consists of fMRI data from twelve individuals (two females), acquired between October 2019 and November 2022. The original cohort comprised thirteen participants, and subject identifiers have remained consistent across releases. The identifiers range from 01 to 15, excluding sub-03 and sub-10, which were never assigned to any participant. One participant (sub-02) withdrew from the study after the first release and therefore did not take part in the tasks included in the present release. Additionally, some participants (sub-01, sub-07 and sub-13) only completed a subset of the acquisitions. The age, sex and handedness of this group of participants are given in Table 1. Handedness was determined with the Edinburgh Handedness Inventory[50].

All experimental procedures were approved by a regional ethical committee for medical protocols in Île-de-France ("Comité de Protection des Personnes" - no. 14-031) and a committee to ensure compliance with data-protection rules ("Commission Nationale de l'Informatique et des Libertés" - DR-2016-033). Every participant granted their informed written consent, according to the Helsinki declaration and the French public health regulation. The consent forms included their agreement for sharing de-identified data in open-access repositories. Participants received compensation of 80 euros per MRI acquisition, with additional fees provided for extra sessions.

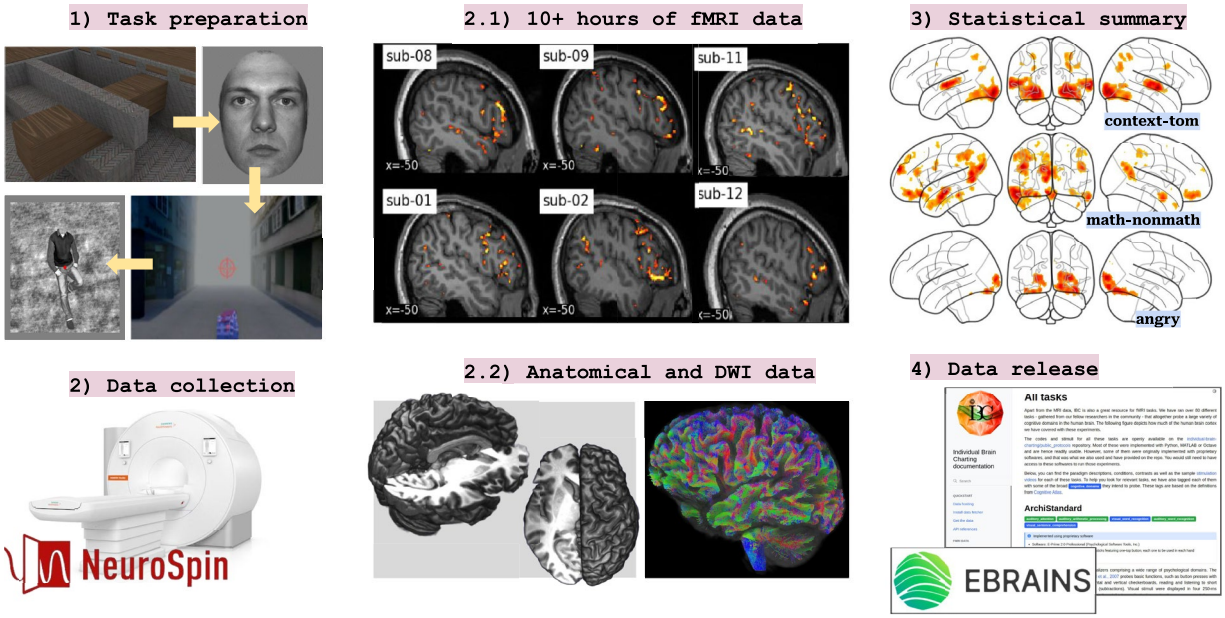

Fig. 1 Overview of the IBC project.Summary of the workflow for this IBC release: **1) Task preparation:** reach out to neuroscience laboratories to integrate their protocols into IBC; replication of scripts and routines. **2) Data collection:** this release comprises 18 tasks and approximately 10 hours of fMRI, adding up to 40 hours with previous releases, along with structural and diffusion-weighted imaging (DWI) data. While DWI was acquired before this release period, the data are included in the release to keep it complete. **3) Statistical summary:** data are preprocessed, and statistical analyses are performed; **4) Data release:** data are released in the hosting platforms, along with and extensive documentation.

Subject ID	Year of recruitment	Age	Sex	Handedness score
sub-01	2015	39	M	0.3
sub-04	2015	26	M	0.8
sub-05	2015	27	M	0.6
sub-06	2015	33	M	0.7
sub-07	2015	38	M	1
sub-08	2015	36	F	1
sub-09	2015	38	F	1
sub-11	2016	35	M	1
sub-12	2016	40	M	1
sub-13	2016	28	M	0.6
sub-14	2016	28	M	0.7
sub-15	2017	30	M	0.9

Table 1. Demographic data of the participants from the current release. Age refers to participant age at the year of recruitment. Acquisitions for this release were performed between October 2019 and November 2022. Note that *sub-02* is also part of the dataset, but did not perform any of the tasks on this release, therefore it is not included in this list. Subject identifiers are consistent across all IBC releases.

MRI Equipment. The fMRI data were acquired using an MRI scanner Siemens 3T Magnetom Prisma^{fit} along with a Siemens Head/Neck 64-channel coil.

Behavioral responses were obtained with two MR-compatible, optic-fiber response devices that were interchangeably used according to the type of task employed: *(1)* a five-button ergonomic pad (Current Designs, Package 932 with Pyka HHSC-1 × 5-N4); and *(2)* a pair of in-house custom-made sticks featuring one-top button. MR-Confon package was used as audio system in the MRI environment.

All sessions were conducted at the NeuroSpin platform of the CEA Research Institute, Saclay, France.

Experimental Paradigms. The tasks were collected from various laboratories within the research community. Most tasks were administered in separate sessions; however, for shorter tasks, participants occasionally completed two or more within the same session. Table 3 presents the distribution of tasks across sessions.

Tasks	sub-01	sub-04	sub-05	sub-06	sub-07	sub-08	sub-09	sub-11	sub-12	sub-13	sub-14	sub-15
BiologicalMotion		ses-29	ses-29	ses-29	ses-29	ses-31	ses-30	ses-30	ses-30	ses-29	ses-29	ses-29
MathLanguage	ses-26	ses-30	ses-35	ses-31	ses-30	ses-17	ses-32	ses-31	ses-31	ses-30	ses-30	ses-30
SpatialNavigation	ses-25	ses-31	ses-30	ses-30	ses-31	ses-15	ses-31	ses-32	ses-32	ses-31	ses-34	ses-31
EmoMem		ses-35	ses-34	ses-35	ses-35	ses-36	ses-36	ses-36	ses-36	ses-35	ses-35	ses-35
EmoReco		ses-35	ses-34	ses-35	ses-35	ses-36	ses-36	ses-36	ses-36	ses-35	ses-35	ses-35
StopNogo		ses-35	ses-34	ses-35	ses-35	ses-36	ses-36	ses-36	ses-36	ses-35	ses-35	ses-35
Catell		ses-36	ses-36	ses-36	ses-36	ses-37	ses-37	ses-38	ses-37	ses-36	ses-36	ses-36
FingerTapping		ses-36	ses-36	ses-36	ses-36	ses-37	ses-37	ses-38	ses-37	ses-36	ses-36	ses-36
VSTMC		ses-36	ses-36	ses-36	ses-36	ses-37	ses-37	ses-38	ses-37	ses-36	ses-36	ses-36
BreathHolding		ses-37	ses-37	ses-37	ses-37	ses-38	ses-38	ses-39	ses-38	ses-37	ses-37	ses-37
Checkerboard		ses-37	ses-37	ses-37	ses-37	ses-38	ses-38	ses-39	ses-38	ses-37	ses-37	ses-37
FingerTap		ses-37	ses-37	ses-37	ses-37	ses-38	ses-38	ses-39	ses-38	ses-37	ses-37	ses-37
ItemRecognition		ses-37	ses-37	ses-37	ses-37	ses-38	ses-38	ses-39	ses-38	ses-37	ses-37	ses-37
VisualSearch		ses-38	ses-38	ses-38		ses-39	ses-39	ses-40	ses-39		ses-38	ses-38
RewProc		ses-39	ses-39	ses-39		ses-40	ses-40	ses-41	ses-40		ses-39	ses-39
NARPS		ses-39	ses-39	ses-39		ses-40	ses-40	ses-41	ses-40		ses-39	ses-39
FaceBody		ses-40	ses-40	ses-40		ses-41	ses-41	ses-42	ses-41		ses-40	ses-40
Scene		ses-40	ses-40	ses-40		ses-41	ses-41	ses-42	ses-41		ses-40	ses-40

Table 2. Tasks in this release performed by each subject. Most of the tasks in this release were performed by a total of 11 subjects; however, there were some subject dropouts over the years. This table provides an overview of the tasks performed by each subject and the corresponding session identifiers, helping to track participation across the dataset.

The following sections provide a detailed description of the paradigms employed for each task, including their experimental conditions and overall organization. Table 4 summarizes each task, the psychological domains it targets, and references to the original studies from which the tasks were adapted. The psychological domains indicate the cognitive processes probed by each task, and are defined according to the *Cognitive Atlas*[44]. Some tasks introduce psychological domains not covered in previous releases, while others extend those already represented in the dataset. This approach reflects our motivation to strengthen the coverage of existing domains while expanding the dataset to include new ones. A complete list of the psychological domains targeted by every regressor of interest is available in Supplementary Table 8.

All materials used for stimulus presentation have been made publicly available, together with video annotations of the corresponding protocols (see Section *Code Availability* Code Availability). Video annotations refer to video records of complete runs that are meant to be consulted for a better comprehension of the task paradigms. These videos can be found on the project's Youtube channel: https://www.youtube.com/@individualbraincharting6314. For each subject, the paradigm-descriptors files describing the occurrence of the events are part of the dataset, following BIDS Specification.

Biological Motion. The *Biological Motion* task that we used was originally developed by[51]. The phenomenon known as "biological motion" was first introduced in[52], and consisted of point-light displays arranged and moving in a way that resembled a person moving.

During the task, the participants were shown a point-light *walker*, and they had to decide if the walker's orientation was to the left or right, by pressing on the response box respectively on the index finger's button or the middle finger's button. The stimuli were divided into 6 different categories: three types of walkers, as well as their reversed versions. The division of the categories focuses on three types of information that participants can obtain from observing the walker: global information, local information, or neither of them.

Global information refers to the general structure of the body and the spatial relationships between its parts. This category of walkers, labeled *global upright* had no informative local cues as to walking direction, and its upside-down counterpart was called *global inverted*. Local information refers to kinematics, speed of the points and mirror-symmetric motion. Within this category, stimuli lacked structural information and were called *natural upright*, with its reversed version labeled *natural inverted*. The third category of walkers didn't contain structural information and was also deprived from acceleration patterns. This category was called *modified upright*, with its upside-down version called *modified inverted*.

We divided the acquisition of this task into two types of runs: runs of type 1 contained stimuli of both global types (upright and inverted) and both natural types, while runs of type 2 contained both natural types and both modified types.

Mathematics and Language (MathLanguage). The *Mathematics and Language* protocol was adapted from[35,53], and aimed to comprehensively capture the activation related to several types of mathematical and other types of facts, presented as sentences.

During the task, the participants were presented with a series of sentences, each one in either of two modalities: auditory or visual. Some of the categories included theory of mind statements, arithmetic facts and

Session	Modality	Task	Duration	Repetitions
BiologicalMotion	2D Spin-Echo	—	00:31	PA(×2) + AP(×2)
	BOLD fMRI	BiologicalMotion1	06:45	PA(×2) + AP (×2)
	BOLD fMRI	BiologicalMotion2	06:45	PA(×2) + AP (×2)
MathLanguage	2D Spin-Echo	—	00:31	PA(×2) + AP(×2)
	BOLD fMRI	MathLanguage (run-01)	09:20	PA
	BOLD fMRI	MathLanguage (run-02)	09:18	AP
	BOLD fMRI	MathLanguage (run-03)	09:30	PA
	BOLD fMRI	MathLanguage (run-04)	09:34	AP
	BOLD fMRI	MathLanguage (run-05)	09:23	PA
	BOLD fMRI	MathLanguage (run-06)	09:24	AP
	BOLD fMRI	MathLanguage (run-07)	09:18	PA
SpatialNavigation	2D Spin-Echo	—	00:31	PA(×2) + AP(×2)
	BOLD fMRI	SpatialNavigation (run-01)	05:00	PA
	BOLD fMRI	SpatialNavigation (runs 02-08)	08:00	PA(×3) + AP(×4)
CamCAN 1	2D Spin-Echo	—	00:31	PA(×2) + AP(×2)
	BOLD fMRI	EmoMem	10:12	PA + AP
	BOLD fMRI	EmoReco	06:25	PA + AP
	BOLD fMRI	StopNogo	10:04	PA + AP
	2D Spin-Echo	—	00:31	PA(×2) + AP(×2)
	BOLD fMRI	Catell	04:30	PA + AP
	BOLD fMRI	VSTMC	08:28	PA(×2) + AP(×2)
	BOLD fMRI	FingerTapping	05:26	PA + AP
FBIRN	2D Spin-Echo	—	00:31	PA(×2) + AP(×2)
	BOLD fMRI	ItemRecognition	07:23	PA + AP
	BOLD fMRI	BreathHolding	06:03	PA + AP
	BOLD fMRI	FingerTap	09:22	PA + AP
	BOLD fMRI	Checkerboard	06:25	PA + AP
VisualSearch	2D Spin-Echo	—	00:31	PA(×2) + AP(×2)
	BOLD fMRI	VisualSearch (run-01)	11:50	PA
	BOLD fMRI	VisualSearch (run-02)	11:48	AP
	BOLD fMRI	VisualSearch (run-03)	11:29	PA
	BOLD fMRI	VisualSearch (run-04)	11:52	AP
NARPS-RewProc	2D Spin-Echo	—	00:31	PA(×2) + AP(×2)
	BOLD fMRI	NARPS	07:23	PA(×2) + AP(×2)
	BOLD fMRI	RewProc	12:03	PA + AP
Scene-FaceBody	2D Spin-Echo	—	00:31	PA(×2) + AP(×2)
	BOLD fMRI	Scene	09:28	PA(×2) + AP(×2)
	BOLD fMRI	FaceBody	07:38	PA(×2) + AP(×2)

Table 3. Details about the MRI-data acquisitions for the sessions that make up this release of the IBC dataset. The table lists the data acqisition sessions that compose this release As each session is dedicated to one or more tasks, the identifier on the *Session* column corresponds to the task name(s) or the name of the task battery. The *Modality* column indicates the type and number of runs acquired for each session. "2D Spin-Echo" refers to the acquisition of field maps with both PA and AP phase-encoding directions. "BOLD fMRI" refers to the acquisition of functional MRI data. The *Task* column indicates the task(s) performed in each session. The *Repetitions* column reports the number of times each run was acquired, along with the corresponding phase-encoding direction (PA or AP). The *Duration* column indicates the length of each run in minutes and seconds. If runs within a tasks had different durations, each duration is listed separately; otherwise, the number of runs with identical duration is indicated in parentheses in the Repetitions column.

geometry facts. After each sentence, the participant had to indicate whether they believed the presented fact to be true or false, by respectively pressing the button with the left or right hand. A second version of each run (runs "B") was generated reverting the modality for each trial, so those being visual in the original runs (runs "A"), would be auditory in their corresponding B version, and vice-versa.

Each participant performed four A-type runs, followed three B-type runs due to time constraints. Each run had an equal number of trials of each category, and the order of the trials was the same for all subjects. The task name was shortened to *MathLanguage* for the task label BIDS specification.

Spatial Navigation. The *Spatial Navigation* protocol, an adaptation from the one used in[36], was originally designed to capture the effects of spatial encoding and orientation learning in different age groups. The task

Tasks	Description	Psychological domains covered	Ref.
BiologicalMotion	Point-light displays arranged and moving in a way that resembled a person walking.	*Existing*: motion detection, response execution, response selection	51,52
	Participants gather information to decide the walker's orientation.	New: biological motion, global motion coherence, local motion coherence	
MathLanguage	Capture activation when presenteded with mathematical and other types of facts presented as sentences either as visual or auditory stimuli.	*Existing*: auditory arithmetic processing, narrative comprehension, visual arithmetic processing	35
		New: auditory geometric processing, visual geometric processing	
SpatialNavigation	Capture the effects of spatial encoding and orientation learning by demanding to navigate and orientate themselves in a complex virtual environment.	Existing: spatial localization, spatial working memory, visual search	36
		New: navigation, spatial memory	
EmoMem	From the CamCAN battery, designed to asses how emotional valence affects implicit and explicit memory.	*Existing*: visual perception	37
		New: imagination, visual cue, positive and negative emotion	
EmoReco	From the CamCAN battery, compares response when observing angry versus response when observing angry versus individuals differ in response regulation.	*Existing*: emotional expression, face perception	37
		New: negative emotion, gender perception	
Catell	From the CamCAN battery, measures activity underpinning fluid intelligence when identifying the "odd one out" from a set of images.	*Existing*: task difficulty, visual form discrimination	37
		New: oddball detection	
FingerTapping	From the CamCAN battery, used to study executive control and action decisions by using visual cues to prompt finger tapping.	*Existing*: response execution, response selection, right finger response execution	37
		New: motor control, motor planning	
VSTMC	From the CamCAN battery, designed to make participants remember size and direction of a dots array and ignore distractors, to asses visual short-term memory.	*Existing*: response execution, response selection, spatial working memory, task difficulty, visual attention	37
StopNogo	From the CamCAN battery, assesses systems involved in action restraint and action cancellation by randomly interleaving "Go", "Stop" and "No-Go" trials.	*Existing*: proactive control, response execution, response inhibition, shape recognition, response selection	37
RewProc	A visual reversal-learning task in which choice of the correct stimulus led to a probabistically determined "monetary" reward and choice of the incorrect led to a monetary loss.	*Existing*: reward processing, risk aversion, cue switch, risk processing, reward valuation	38,54
		New: loss aversion, color perception, repetition	
NARPS	Mixed gambles task for studying the neural basis of loss aversion and whether subjects tend to be more sensitive to losses as compared to equal-sized gains.	*Existing*: risk processing, risk aversion, reward processing, response selection	39,55
		New: decision making, reward anticipation loss aversion	
FaceBody	Used to define category-selective cortical regions that respond preferentially to faces, places, bodies, or printed characters.	*Existing*: body, face and place maintenance, body, face and place recognition	40
		New: object maintenance, visual letter, number and object recognition	
Scene	Designed to study how the brain combines spatial elements to form a coherent percept. Participants judged whether presented scenes were possible.	*Existing*: spatial attention, lower left and right vision, salience, visual scene perception	41
		New: oddball detection	
BreathHolding	Part of the FBIRN battery, designed to measure vascular response and its effect n the BOLD signal.	*New*: self monitoring, breath holding	42
Checkerboard	Part of the FBIRN battery, block design sensorimotor task with alternating 16s long blocks of rest and visual stimuli with a checkerboard.	*Existing*: visual perception, response selection, response execution	42
FingerTap	Part of the FBIRN battery, reaction time task in which subjects press one of the four keypad buttons when they see a corresponding visual cue.	*Existing*: response execution, selection, finger response execution	42
ItemRecognition	Part of the FBIRN battery, working memory task with different loads, consisting of memorizing a set of targets and then respond whether the shown probe is a target.	*Existing*: numerosity, spatial working memory, task difficulty, visual attention	42
VisualSearch	Aims to study the mechanism underlying the spatially specific activation of sensory codes while searching for a visual or remembered target.	*Existing*: visual form discrimination, visual working memory, visual search, visual pattern recognition	43,56
		New: working memory maintenance	

Table 4. Overview of the tasks featuring this IBC release. Brief description of each task, the psychological domains it covers, and references to the original studies from which the tasks were adapted. The psychological domains marked as *Existing* have been covered in previous IBC releases, while those marked as *New* are introduced in this release.

demanded subjects to navigate and orient themselves in a complex virtual environment that resembled a typical German historic city center, consisting of town houses, shops and restaurants. There are three parts of this task: introduction (outside of the scanner), encoding (in scanner) and retrieval (in scanner). Before entering the scanner, participants went through an introduction phase, during which they had the freedom to navigate the virtual environment with the objective of collecting eight red balls scattered throughout various streets of the virtual city. During this part, the participants could familiarize themselves with the different buildings and learn

IBC release	Tasks featured
First release[11]	ArchiStandard, ArchiSpatial, ArchiSocial, ArchiEmotional, HcpEmotion, RSVPLanguage, HcpGambling, HcpMotor, HcpLanguage, HcpRelational, HcpSocial, HcpWm,
Second release[12]	PreferenceFood, PreferencePaintings, PreferenceFaces, PreferenceHouses, MTTWE, MTTNS, TheoryOfMind, VSTM, Enumeration, EmotionalPain, PainMovie, Self, Bang
Third release[24]	Clips, WedgeClock, WedgeAnti, Ring, Raiders
Fourth release	Lec1, Lec2, Audi, Visu, MVEB, MVIS, Moto, MCSE, Audio, Attention, DotPatterns, StopSignal, SelectiveStopSignal, TwoByTwo, Discount, ColumbiaCards, Stroop, WardAndAllport
Fifth release (this manuscript)	BiologicalMotion, MathLanguage, SpatialNavigation, EmoMem, EmoReco, Catell, FingerTapping, VSTMC, StopNogo, RewProc, NARPS, FaceBody, Scene, BreathHolding, Checkerboard, FingerTap, ItemRecognition, VisualSearch

Table 5. Overview of the tasks featured in each IBC release. The table shows the tasks included in each release of the IBC project. Each task is labeled according to the naming convention used in the IBC documetation, which is consistent with the naming in the released files. We have organized the data across these five releases to enhance the readability of the different data descriptors, make the data available as soon as possible, and allow for the inclusion of new tasks as they become available. The final, sixth release will follow after the present one.

the location of the two target buildings: Town Hall and Church. After they had collected all the red balls, a short training of the main task was performed to ensure the correct understanding of the instructions.

Then, participants went to the scanner. The task began with the encoding phase. During this period, the participant had to passively watch the camera move from one target building to the other, in such a way that every street of the virtual environment is passed through in every direction possible. Participants were instructed to pay close attention to the spatial layout of the virtual environment and the location of the target landmarks. Passive transportation instead of self-controlled traveling was chosen to ensure that every participant experienced the virtual environment for the same amount of time.

After, the retrieval phase started. In each trial, the participant was positioned near an intersection within the virtual environment, which was enveloped in a dense fog, limiting visibility. Subsequently, the camera automatically approached the intersection and centered itself. There were two types of trials on the retrieval phase: experimental and control trials. During experimental trials, one of the two target buildings (Town Hall or Church) was displayed as a miniature picture at the bottom of the screen. The participant's task was to indicate the direction of the target building, relative to their current position at the intersection, by pointing with the response box to one of the buildings of the intersection. During control trials, no target building was shown. The participant had to point to one of the buildings of the intersection that had been colored in blue, instead of the target building. The retrieval phase consisted of 8 experimental trials and 4 control trials per run.

All of the runs, except the first one, began with the encoding phase, followed by the retrieval phase. In the initial run, a control trial of the retrieval phase preceded the standard design of the encoding phase followed by the retrieval phase.

CamCAN battery. The *Cambridge Centre for Ageing and Neuroscience (CamCAN)* battery consists of a set of protocols designed to understand how individuals can best retain cognitive abilities into old age[37]. All modifications for adapting the battery into IBC were done taking care not to alter the psychological state that the original tasks were designed to capture. From this battery, the following tasks were included in IBC: *Emotional Memory*, *Emotional Recognition*, *Stop-NoGo*, *Catell - Oddball*, *Finger Tapping* and *Visual and Spatial Memory*.

Emotional Memory (EmoMem). The EmoMem task was designed to assess implicit and explicit memory, and how it is affected by emotional valence. In each trial, participants were presented with a background picture for 2 seconds, followed by a foreground picture of an object superimposed on it. Participants were instructed to imagine a "story" linking the background and foreground pictures, and after an 8-second presentation, the next trial began. The manipulation of emotional valence exclusively affected the background image, which could be negative, neutral, or positive. Participants were asked to indicate the moment they thought of a story or a connection between the object and the background image by pressing a button. The task name was shortened to *EmoMem* for the task label BIDS specification.

Emotional Recognition (EmoReco). The *Emotional Recognition* task compares brain activity when observing angry versus neutral expressions, and assesses how individuals differ in how they regulate responses to negative emotional expressions. The expressions were presented on female and male faces (15 each), and each face had an angry and a neutral expression version. Emotions were presented in blocks of angry and neutral, with equal numbers of female and male faces in each block. In each trial, participants were asked to press one button for male faces and another for female faces. The task name was shortened to *EmoReco* for the task label BIDS specification.

Stop-NoGo. The *Stop-NoGo* task assesses systems involved in action restraint and action cancellation, by randomly interleaving *Go*, *Stop* and *No-Go* trials. On *Go* trials, participants viewed a black arrow pointing left or right for 1000 ms, and had to indicate the direction of the arrow by pressing the left/right buttons with their right hand. On *Stop* trials, the black arrow changed color from black to red, after a short variable stop-signal delay. Participants were instructed not to respond to the red arrow, so stop signal trials required canceling the initial response to the black arrow. The Stop-Signal delay varied trial-to-trial in steps of 50 ms, and a staircase

procedure was used to maintain a performance level of 66% successful inhibition. Finally, in *No-Go* trials, the arrow was colored in red since the start of the trial (stop-signal delay of 0) and participants were required to make no response.

Catell. The *Catell* task was used to provide a measure of neural activity underpinning fluid intelligence. In each trial, participants were shown a set of 4 images and were asked to identify the "odd one out". While some trials presented easily identifiable differences between the oddball and the other images, others were more challenging, requiring participants to detect abstract patterns to identify the oddball. Participants completed alternating blocks of easy and difficult trials, each lasting 30 seconds. In total, they performed four blocks of easy problems and four blocks of difficult problems. In each trial, a stimulus appeared on the screen and remained until the participant responded, with the block automatically ending after 30 seconds and the next block beginning immediately. Participants were encouraged to take as much time as needed and were advised to respond only when confident in their answers. This design led to variable number of trials per block among individuals, while maintaining a consistent duration for each type of problem (easy and difficult).

Finger Tapping. The *Finger Tapping* task was originally designed to study executive control and action decisions in aging and neurodegenerative diseases. Participants were presented with an image of a right hand and were instructed to press a button with one of their four right-hand fingers in response to a cue. The cue was either a "specified" cue in which a single opaque circle indicated which finger to press, or a "chosen" cue in which 3 circles appeared opaque indicating that participants must choose one of the 3 opaque fingers to press. Cues were presented for 1 second with a stimulus onset asynchrony of 2.5 seconds, and were pseudorandomly ordered so that participants did not see four or more responses of the same condition (action selection, specified or null) in a row.

Visual Short-Term Memory (VSTMC). The *Visual Short-Term Memory* task was designed to assess the neural process underlying visual short-term memory. In each trial, participants saw three arrays of colored dots: one red, one yellow, and one blue. The dot displays were presented in rapid succession beginning with a 250 ms fixation period followed by a 500 ms presentation of the dot display. To manipulate set size, one, two, or three of the dot displays moved in a single direction, which had to be remembered. The remaining displays rotated around a central axis and served as distractors, which had to be ignored. After the presentation of the third display, an 8-second delay followed, during which participants had to remember the direction(s) of motion for the non-rotating dots. Subsequently, the probe display appeared, with a colored circle indicating which dot display to recall (red, yellow, or blue). Within the circle, there was a pointer that had to be adjusted to indicate the direction in which the target dot display had been moving. Participants were given 5 seconds to adjust the pointer to match the direction of the to-be-remembered dot display. On 90% of trials the probed movements were in one of three directions: 7, 127, or 247 degrees.

Reward Processing (RewProc). The *Reward Processing* task was adapted from[38] and[54]. The protocol aimed at discerning the role of the orbito-frontal cortex (OFC) using a similar to emotion-related visual reversal-learning task in which the choice of the correct stimulus led to a probabilistically determined monetary reward and the choice of the incorrect stimulus led to monetary loss.

In each trial of a run of this protocol, two unfamiliar and easily distinguishable fractal patterns were displayed on a gray background, positioned to the left and right of a central fixation cross. At the beginning of the task, one of the patterns was arbitrarily designated as the "correct" option, while the other was designated as "incorrect". The task for the participants was to select one of these two patterns. Selecting the correct pattern led to a monetary gain with a 70% probability, and a monetary loss with a 30% probability. Selecting the incorrect pattern led to a monetary gain with a 30% probability and a monetary loss with a 70% probability (reversed gain-loss probability contingencies). After selecting either pattern, a black box appeared around the chosen pattern, followed by feedback indicating the amount of symbolic money (either 20 or 10 units) that was gained or lost in the particular trial which could be either 20 or 10 units. The probability of receiving either 10 or 20 units of money was equal. Furthermore, if the participant consecutively selected the correct pattern for a specified criterion, i.e. 5 consecutive times, a reversal of the gain-loss probability contingencies occurred after a Poisson process. This meant that there was a 25% probability that a reversal took place in the gain-loss probabilities on any post-criterion trial.

The timing of trial events in the IBC implementation of the task differed from those in the two aforementioned studies. This adjustment was made after a discussion with the initial protocol authors, who considered that the timing in the final IBC-implementation version was more appropriate for achieving adequately separated events to minimize temporal correlations while maintaining a reasonable total trial length. Specifically, the pre-fixation cross was displayed for a duration ranging from 500 to 1500 ms. The stimuli remained on the screen for less than 3000 ms for participant selection, and the outcome feedback was presented with a 1750 ms delay, lasting for 1750 ms.

The task name was shortened to *RewProc* for the task label BIDS specification.

Function Biomedical Informatics Research Network battery (FBIRN). The *Function Biomedical Informatics Research Network* (FBIRN) battery of protocols[42] was designed to assess the major sources of variation in fMRI studies conducted across scanners, including instrumentation, acquisition protocols, challenge tasks, and analysis methods. All modifications were done taking care to not alter the psychological state that the original

tasks were designed to capture. From this battery, the following tasks were included in IBC: *Breath Holding*, *Checkerboard*, *Finger Tap* and *Item Recognition*.

Breath Holding. The *Breath Holding* task was designed to measure vascular response. In a block design, participants alternated between breathing normally for 20 seconds and holding their breath for 16 seconds. They were given a warning 2 seconds before the hold breath signal was presented, so they could prepare to hold their breath. No response was required in this task.

Checkerboard. The *Checkerboard* protocol is a block design sensorimotor task with alternating 16-second long blocks of rest and visual stimulation with a checkerboard stimulus. In the checkerboard block, a checkerboard filling the visual field was presented for a period of 200 ms at random intervals (avg. ISI = 762 ms, range: 500-1000 ms), and the subject pressed a button each time the checkerboard appeared on the screen. The run started and ended with fixation blocks, and 11 blocks of checkerboard stimulation were presented.

Finger Tap. The *FingerTap* protocol is a block design reaction time task in which participants pressed one of the four keypad buttons when they saw a corresponding visual cue ('1' for button 1, '2' for button 2, ..., '4' for button 4). The stimuli appeared at 1-second intervals and subjects got 2 seconds to make their response. The task blocks were interleaved with rest blocks lasting 15 seconds.

Item Recognition. The *Item Recognition* protocol is a working memory (WM) task where subjects had to remember items with a varying load of 1, 3 or 5 items. There were four conditions in this task; on three of them, participants were shown series of either one, three or five targets (digits), displayed in red, and were asked to memorize them. They were then presented with probes (also digits) displayed in green, and were required to indicate whether the probe matched one of the targets or not.

In the fourth condition, participants were shown a series of arrows and were asked to indicate the direction of the arrows (left or right).

This task followed a block-design format with 2 blocks for each of the 3 Working Memory conditions, along with 2 blocks for the arrow condition.

Neuroimaging Analysis Replication and Prediction Study (NARPS). This protocol is more commonly known as the mixed gambles task and was adapted from the *Neuroimaging Analysis Replication and Prediction Study* (NARPS)[39]. The study aimed to estimate the variability of neuroscientific results across analysis teams. The mixed gambles task is originally from[55] and studied the neural basis of loss aversion, which is the phenomenon that suggests that people tend to be more sensitive to losses as compared to equal-sized gains. The study investigated whether potential losses elicit negative emotions, which then drive loss aversion or rather the same neural systems, encoding subjective value, asymmetrically respond to losses compared to gains.

Participants were presented with a mixed gamble where they had a 50% chance of either gaining one amount of symbolic money or losing another amount. The possible gains and losses both ranged between 5-20 units (equal range condition), in increments of 1 unit and all 256 possible combinations of gains and losses were presented to each participant in the same sequence. The stimulus consisted of a circle presented on a gray screen and divided into two halves: on one side the gain amount was presented in green with a plus (+) sign before the number, and on the other side the loss amount was presented in red with a minus (−) sign before the number. Participants were then asked to decide whether or not they would like to accept the gambles presented to them, with four possible responses for each gamble: strongly accept, weakly accept, weakly reject or strongly reject. The gamble was presented on the screen until the participant responded or four seconds had passed, followed by a grey screen until the onset of the next trial.

The task label used for the BIDS specification was *NARPS*.

Face Body. This protocol was adapted from[40], where it was used to expose category-selective cortical regions that respond preferentially to faces (e.g., fusiform face area), places (e.g., para-hippocampal place area), bodies (e.g., extrastriate body area), or printed characters (e.g., visual word form area). A detailed description and code for the original protocol is available in github: https://github.com/VPNL/fLoc. In the IBC implementation of the protocol, participants were presented with images from five categories, each associated with two related subcategories:

- Faces: adult faces and children faces
- Places: corridors and houses
- Bodies: full bodies without faces and just limbs
- Objects: cars and instruments
- Characters: numbers and words

The protocol used a mini-block design in which 12 stimuli of the same subcategory were presented in each block. The sequence of the blocks was randomized over the ten subcategories and a blank baseline condition, and each subject was presented with the same sequence. In total, there were 144 images per subcategory. To ensure that the subjects remained alert throughout the experiment, they were asked to press a button when an image is repeated as a mirrored image (flipped 1-back task).

Scene. This protocol was adapted from[41], and was designed to identify how the brain combines spatial elements to form a coherent percept. To this end, participants judged whether Escher-like scenes were possible or impossible.

56 scenes were designed for the original study that appeared spatially incoherent when viewed from a particular angle and were termed *impossible scenes*. Possible counterparts were created for each impossible scene, and these were termed *possible scenes*. For comparison, baseline non-scene images were created by scrambling the scenes and matched for low-level visual properties. A partially transparent circle was overlaid at a pseudo-random location on each of the scrambled scenes, such that half of these dots were found on the left and half on the right of the baseline scrambled images. On these scrambled image dot trials, participants indicated the left/right location of the dot. There were easy and hard versions that depended on the transparency of the overlaid circle.

Visual Search, Working Memory (VisualSearch). This protocol was adapted from[43], who aimed to elucidate the neurophysiological mechanism underlying the spatially specific activation of sensory codes while searching for a visual or remembered target. A set of eight stimuli items was selected from a set of 100 novel and difficult to verbalize closed shape contours previously developed by[56] in the original as well as in the IBC implementation of the study.

Each run of the protocol involved two kinds of trials - visual search and working memory search. In visual search trials, the participants were first shown an abstract item (sample item) and then they had to search for that item in a set of two or four items (search array). In the working memory search trials, the participants were first shown a set of two or four items (memory array) and then they had to tell whether a subsequently shown item (probe item) was present in the previously shown set of items. Thus, in addition to the type of search (visual or working memory) and search response (target present or absent), the array load (two or four items) was also varied in each trial.

In the original study, the participants also performed a separate session for a visual localizer task, where they viewed the stimuli passively without making any responses. This session was excluded from the IBC implementation of the protocol. Furthermore, the response period was also increased from 1000 ms to 2000 ms and the stimuli size from 1.72 to 1.80 degrees of visual angle, following the feedback from pilot sessions.

The task name was shortened to *VisualSearch* for the task label BIDS specification.

Data Acquisition. We have carefully ensured that acquisition conditions and processing pipelines remain as consistent as possible across sessions throughout time. For this reason, some sections, such as *Imaging Data Acquisition*, *Preprocessing*, *Model Specification*, *Model Estimation* and *Summary Statistics* are identical to those described in previous releases, (see Pinho *et al.* 2018[11]), but are included here for completeness.

Preparation. Upon arrival at NeuroSpin, participants were instructed on the execution and timing of the tasks for the upcoming session. The session identifier may differ from subject to subject, depending on the order of task acquisition and individual constraints. Once a year, participants underwent different medical tests, including a general physical examination, a blood test and a urine test, to ensure their overall health status. However, those measurements are not released as part of the dataset. Tasks were not repeated across sessions. Table 3 provides an overview of the session structure and details the tasks undertaken by each participant. Data anomalies are mentioned in Supplementary Table 6.

Imaging Data Acquisition. Details in this section are identical to those described in previous releases (see Pinho *et al.*[11]), but are repeated here to ensure completeness.

FMRI data were collected using a *Gradient-Echo* (GE) pulse, whole-brain *Multi-Band* (MB) accelerated[57,58]*Echo-Planar Imaging* (EPI) T2*-weighted sequence with *Blood-Oxygenation-Level-Dependent* (BOLD) contrasts. For each protocol, runs were equally divided between *Posterior to Anterior* (PA) and *Anterior to Posterior* AP phase-encoding directions, with the order of the phase-encoding directions being counterbalanced across runs. The main purpose was to ensure within-subject replication of the same task, while mitigating potential limitations concerning the distortion-correction procedure.

Spin-Echo (SE) EPI-2D image volumes were acquired in order to compensate for spatial distortions. Similarly to the GE-EPI sequences, two different phase-encoding directions, PA and AP, were used in different runs. In every session, one pair of PA and AP *SE EPI-2D* volumes was acquired before the task (*GE-EPI* sequences), and another pair was acquired at the end.

Behavioral Data. Active responses were required from the participants in all tasks except for the Breath Holding task. The registry of all behavioral data, such as the qualitative responses to different conditions and corresponding response times were held in log files generated by the stimulus-delivery software. Supplementary tables from section *Behavioral Data* provide the individual scores for every run and the average across runs for each task.

Data Analysis. *Preprocessing.* Details in this section are identical to those described in previous releases (see Pinho *et al.* 2018[11]), but are repeated here to ensure completeness.

Images were converted to NIfTI format using the*dcm2nii* tool[59]. Following, the NIfTI images were de-identified: pseudonyms were removed and images were defaced using the `mri_deface` tool from the

Freesurfer-6.0.0 library[60]. Data were preprocessed using PyPreprocess: https://github.com/neurospin/pypreprocess, a Python-based tool for running precompiled functions from the *SPM12* software package and the *FSL* library (v5.0)[61]. For each session, the susceptibility-induced off-resonance fields were estimated from four SE EPI-2D volumes, acquired in pairs with opposite phase-encoding directions (PA and AP). The images were corrected using the estimated deformation model with the *topup* tool[62], implemented in FSL. Following this correction, GE-EPI volumes for each participant were aligned using a rigid-body transformation, using the average volume across runs as reference[63]. The mean EPI volume was co-registered to each participant's T1-weighted *MPRAGE* anatomical image[64]. Both anatomical and functional data were then normalized to the standard *MNI152* space using the *Unified Segmentation* probabilistic framework[65].

Model Specification. Details in this section are identical to those described in previous releases (see Pinho *et al.* 2018[11]), but are repeated here to ensure completeness.

fMRI data were analyzed using the General Linear Model (GLM). Regressors of interest were defined to capture variations in the BOLD signal associated with each task condition, reflecting neuronal activity related to task performance[66,67]. Supplementary Table 7 provides a complete description of all regressors of interest included in the models for each task. In addition, nuisance regressors were modeled to account for spurious effects during acquisition, such as variability in the HRF peak latency, head motion, physiological noise and slow drifts within run. The GLM was implemented using *Nilearn* (v0.9.0)[68].

Model Estimation. Details in this section are identical to those described in previous releases (see Pinho *et al.* 2018[11]), but are repeated here to ensure completeness.

To restrict GLM parameter estimation to voxels within functional brain regions, a brain mask was extracted from the normalized mean GE-EPI volume thresholded at 0.25, using Nilearn. This corresponds to a 25% average probability of observing gray matter in a voxel across subjects. A mass-univariate GLM was then applied to the preprocessed EPI data for every run and every task using *Nilearn*. A spatial smoothing kernel of 5 mm full-width at half maximum (FWHM) was applied as a regularization term. Parameter estimates for all regressors in the model, along with their covariance, were computed at every voxel. Linear contrasts between regressors of interest and the baseline were then performed to obtain statistical contrast maps of the evoked responses. The GLM implementation and subsequent statistical analyses were performed with *Nilearn*.

Summary Statistics. Details in this section are identical to those described in previous releases (see Pinho *et al.* 2018[11]), but are repeated here to ensure completeness.

Since data were collected for each task and subject in at least two acquisitions with opposite phase-encoding directions, statistics of their joint effects were computed using a *Fixed-Effects* (FFX) model. At every voxel, *t*-tests were then performed for each individual contrast to assess statistical significance of the evoked response differences. To ensure standardized results independent of the number of observations, *t*-values were directly converted into *z*-values. The resulting derivatives are provided as individual contrast maps containing standard *z*-scores across all voxels within the gray matter mask described above. A list of the main contrast maps available for each task is provided in Supplementary Table 9.

Data Records

EBRAINS Knowledge Graph[69] is the main repository of the IBC project, as it complies with the European regulations on General Data Protection Regulation (GDPR) and the principles of the FAIR data management[70]. Users can access the data via the *EBRAINS Knowledge Graph* after creating an account with an institutional email address.

The dataset is released in cumulative versions, with each version including data from previous releases. Version `v4.0` comprises up to 65 tasks, incorporating those added in this release. The repository is organized into thirteen main directories: `sub-01` to `sub-15`. Note that `sub-03` and `sub-10` are not part of the dataset, as these IDs were never assigned. The directories for `sub-01`, `sub-07` and `sub-13` contain data up to their final completed sessions, since these participants performed only a subset of the tasks from this release. In contrast, `sub-02` did not take part in any of the tasks described here. Nevertheless, their directory in the IBC collection still includes data from earlier sessions up to their last participation. Specifically, `sub-07` and `sub-13` performed all tasks except *FaceBody*, *NARPS*, *Scene*, *Reward Processing*, and *VisualSearch*; while `sub-01` only performed the *MathLanguage* and *Spatial Navigation* tasks in this release.

Data from each subject are numbered on a per-session basis, following the chronological order of the acquisitions; note that session numbering is subject-specific. The exact correspondence between session number and session id for every subject can be found in Table 2.

Source data. Raw data are available on the EBRAINS repository under https://doi.org/10.25493/S7GR-CT0[71]. Different identifiers are assigned to different types of data following the BIDS specification:

- g-zipped NIfTI 4D image volumes of BOLD fMRI data are named as `sub-XX_ses-YY_task-ZZZ_dir-AA_bold.nii.gz`, in which `XX` and `YY` refer respectively to the subject and session id, `ZZZ` refers to the task name, and `AA` can be either 'PA' or 'AP' depending on the phase-encoding direction
- event files are named as `sub-XX_ses-YY_task-ZZZ_dir-AA_event.tsv`
- single-band, reference images are named as `sub-XX_ses-YY_task-ZZZ_dir-AA_sbref.nii.gz`

Each collection contains several *json* files:

- A *json* file for each task in the version, containing acquisition parameters such as *Repetition Time, Echo Time, Flip Angle, Slice Timing, Multiband Acceleration Factor, Software Version*, and details about the place of acquisition. Each file is named as `task-ZZZ_dir-AA_MMM.json`, where `ZZZ` refers to the task name, `AA` can be either 'PA' or 'AP' depending on the phase-encoding direction, and `MMM` can be either 'bold' or 'sbref' for the sequences of the task acquisition or the single-band reference image acquisition.
- A *json* file for each sequence run during different sessions, providing information about the *Phase Encoding Direction* and *Total Readout Time*.

Additionally, a `README.md` and a `participants.tsv` file are included. The former provides a dataset content overview and the latter contains information about the sex, age and handedness of each subject.

Preprocessed data. Preprocessed data are available on the EBRAINS repository under DOI **10.25493/4ZZ6-5S5**[72]. The directory tree structure was similar to that of source data. Different identifiers are assigned to different types of data, as follows:

- gzipped NIfTI 4D image volumes of preprocessed BOLD fMRI data are named as `sub-XX_ses-YY_task-ZZZ_dir-AA_space-MNI152NLin2009cAsym_desc-preproc_bold.nii.gz`, in which `XX` and `YY` refer respectively to the subject and session id, `ZZZ` refers to the name of the task, and `AA` can be either 'PA' or 'AP' depending on the phase-encoding direction. The suffix `_space-MNI152NLin2009cAsym` indicates that the data is in the standard MNI152 space
- event files are named as `sub-XX_ses-YY_task-ZZZ_dir-AA_event.tsv`;
- time series files are named as `sub-XX_ses-YY_task-ZZZ_dir-AA_desc-confounds_timeseries.tsv`, and contain the time series of the nuisance regressors used in the GLM analysis;

Additionally, the repository contains a similar set of *json* files for all tasks and acquisitions as the *Source Data* repository. Moreover, the collection also contains a version of the preprocessed data that have been resampled at 3-millimeter isotropic resolution (the acquisition resolution and the resampling resolution after normalization were both 1.5mm isotropic). This version is available on EBRAINS under DOI **10.25493/DTEX-HWU**[73]. The data organization is the same as the original preprocessed data.

Derived statistical maps. Statistic contrast maps are available on the EBRAINS repository under DOI **10.25493/873R-QK2**[74]. The NIfTI files as well as paradigm descriptors and imaging parameters are organized in two main directories:

- `resulting_smooth_maps`, containing statistical volumetric maps organized through subjects ans sessions, as the source and preprocessed data.
- `resulting_smooth_maps_surface`, containing statistical surface maps organized through subjects ans sessions, as the source and preprocessed data.

Supplementary Tables. All supplementary tables are available on Figshare[75].

Online Documentation. The online documentation is available following the link: https://individual-brain-charting.github.io/docs/. Users can find at any moment the information detailed in this manuscript, including description of the tasks across releases, acquisition parameters, and guidelines on where and how to get the data in a user-friendly manner.

Technical Validation

Data quality. To estimate the quality of the data, we performed several measurements. The results are presented in Fig. 2.

- **Temporal Signal-to-Noise Ratio (tSNR):** Following (Murphy *et al.*)[76], tSNR was calculated as the mean of each voxel's time course divided by its standard deviation, using normalized and unsmoothed data averaged across all acquisitions. As shown in Fig. 2 (panel *a*), tSNR values are higher than 50 in most of the cortex, indicating good signal quality given the high resolution (1.5mm isotropic).
- **Motion Estimates:** The histogram of the six rigid-body motion estimates per scan (three translations in mm and three rotations in degrees) is shown along with their 99% coverage interval in Figure 2 (panel *b*). Motion is typically confined within $[-1.1, 1.5]$ mm/degrees, and values exceeding 1.5 are rare. No acquisitions were discarded due to excessive motion (>2 mm/degrees).
- **Framewise displacement (FD):** FD, as defined by (Power *et al.*)[77], was calculated from the six rigid-body motion estimates across runs for each task and subject. Figure 2 (panel *c*) shows the 90th-percentile FD distribution across all acquisitions. In most cases, FD values are below 0.5 mm, which is considered as acceptable in the field's practice.

Effect of subject identity, task stimuli and phase-encoding direction on activation maps. We assessed how much variability in the signal could be explained by three factors: the effect of *(1)* subject identity,

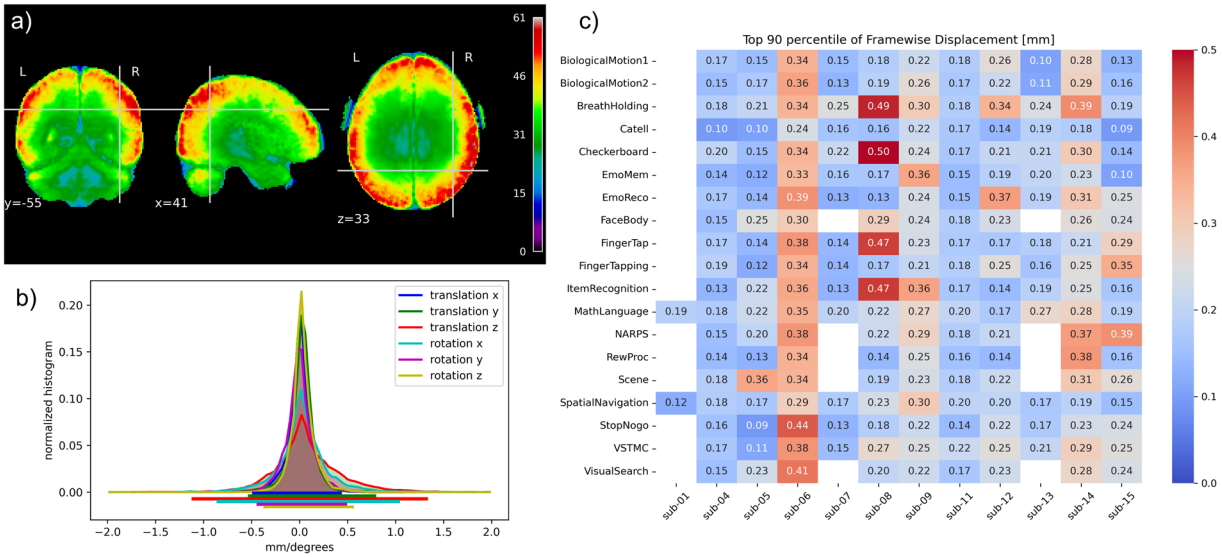

Fig. 2 Global quality of the acquired data. **(a)** Temporal Signal to Noise Ratio (tSNR) map averaged across all subjects and tasks. As we reach the cortex, values gradually increase, getting to a range between 40 and 65, with larger tSNR in cortical regions. **(b)** Density of within-run motion parameters, pooled across all subjects and all tasks. Six distributions are plotted, for the six rigid-body parameters of head motion (translations and rotations are in mm and degrees, respectively). Bold lines below indicate the 99% coverage of all distributions and show that motion parameters mostly remain confined to 1.5mm/1degree across 99% of all acquired images. **(c)** Frame-wise displacement (FD) across acquisitions. The heat map shows the 0.9 quantile of the FD distribution across the tasks in this release. Each distribution is based on the EPI volumes corresponding to all time frames for all acquisitions. The Biological Motion task was split into two sub-tasks due to variations in stimuli and task design. As subjects sub-07 and sub-13 were not available for further acquisitions, their last session was for the FBIRN battery, which explains the white spots on the heat map. Sub-01 only performed two tasks in this release, thus only two values are displayed.

(2) condition and *(3)* phase-encoding direction. This was done by analyzingGLM outputs for each acquisition at every voxel. A one-way *Analysis of Variance* (ANOVA) was performed on all contrast maps ($n = 2042$ from 12 subjects, after removing duplicates). The resulting statistical maps are shown in Fig. 3. Results show that the effects of subject identity and condition are both uniformly significant ($p < 0.05$, FDR corrected). Condition effects are predominantly higher than subject effects, specially in sensory regions, like the visual and auditory cortex. This is expected, as experimental conditions were designed to capture the largest share of task-related signal. By contrast, the effect of the phase-encoding direction is mostly present on regions with high susceptibility to distortions, such as the frontal and occipital cortex. However, the effects are weaker compared to those of subject and condition.

Brain Coverage. Figure 4 shows the brain coverage of this release of the IBC dataset. It displays all brain areas significantly involved in response to the tasks on this release, which was calculated by computing the *Stouffer's Z-score* across all contrast maps. We chose this metric since it is a standard method to combine p-values from each independent statistical tests[78].

Overall, in this release the tasks collectively encompass most cortical and subcortical regions. Notably, the strongest effects are observed in the occipital cortex. We also see larger effects in the cerebellum when compared to the previous release, which is now more uniform across the cerebellar cortex. Meanwhile, the coverage of regions in the motor and sensory cortex appears visually lower, as shown in Fig. 4 (compared to Figure 1 in[12]). This is expected since the tasks on this release do not involve explicit motor responses further than button presses. Nevertheless, it is important to note that the coverage of these regions remains statistically significant, and the cumulative effect of coverage across releases contributes to our overall goal of achieving comprehensive brain coverage while accounting for MR-related constraints, given that some locations benefit from more coil sensitivity.

Behavioral Data. Most tasks in this release required participant responses, with the exception of the *Breath Holding* task. These responses were collected and used to calculate performance scores, providing an estimate of task engagement and attentiveness throughout the acquisitions. Such measures serve as a reference for assessing data reliability. Individual scores for each run, as well as averages across runs for every task, are provided in the supplementary material. Below, we describe the meaning of each score and the method used for its calculation. The tasks *Biological Motion*, *Checkerboard* and *FingerTap* did request active responses from the participants, but the responses were not recorded. Therefore, we were not able to calculate scores for these tasks. Figure 5 summarizes the distribution of individual scores for each task using boxplots.

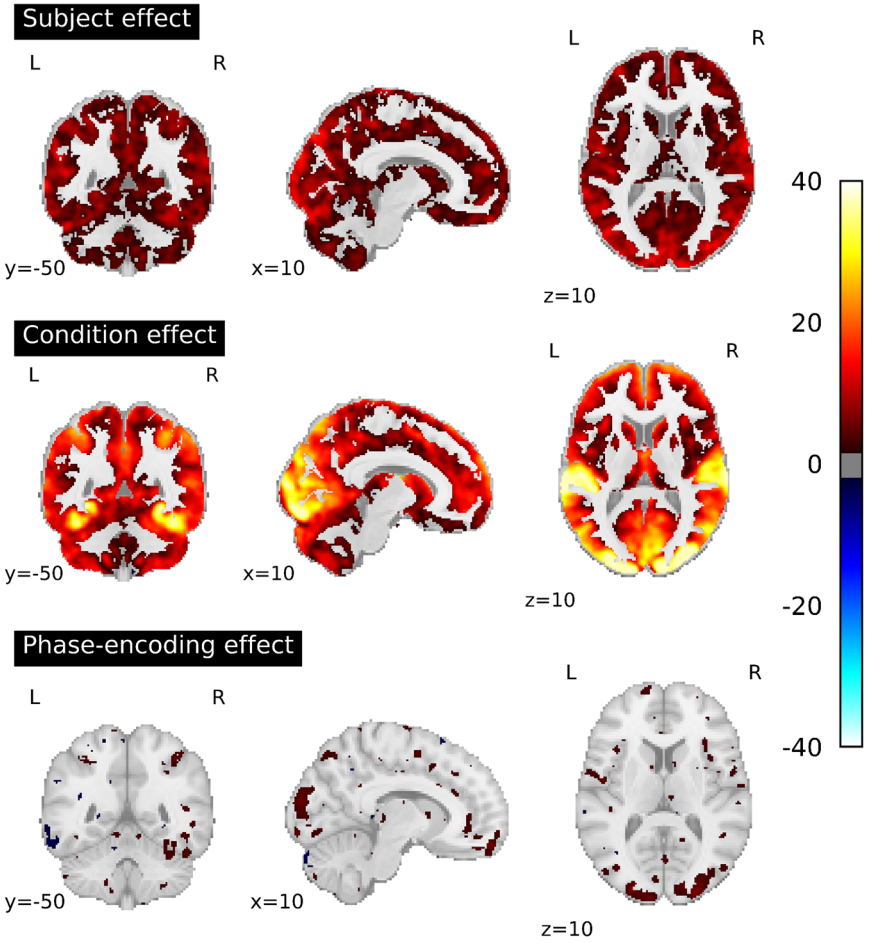

Fig. 3 Voxel-wise variance analysis.Results of a per-voxel ANOVA showing how the variance in activation maps is explained by **(top)** subject identity, **(middle)** task condition, and **(bottom)** phase-encoding direction.

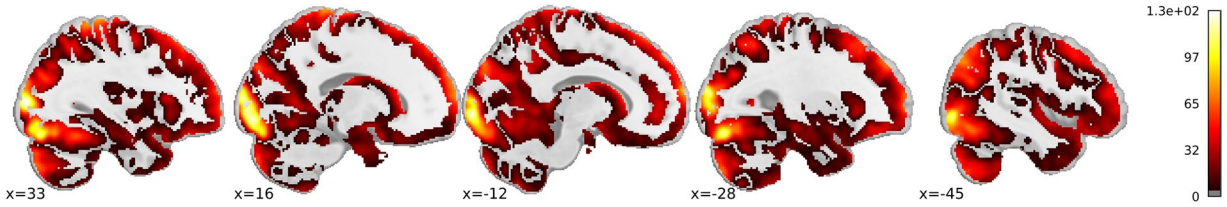

Fig. 4 Brain coverage of this IBC-dataset release.Group-level F-map, at a threshold of $p < 0.05$, Bonferroni-corrected, representing the total area of the brain significantly covered by the tasks featuring in this release of the IBC dataset (FFX across tasks and subjects). It is noticeable that the occipital cortex shows the highest effects, complementary to that of previous releases.

Mathematics and Language. Scores were calculated as the number of correctly classified statements (maximum of 64 per run). Missed responses were counted as incorrect, and chance level was 50%. Supplementary Table 10 provides the individual scores for every run and the average across runs.

Spatial Navigation. Scores were narrowed down to whether the subject pointed to the correct cardinal direction, as if their error was within 45 absolute degrees of the correct direction, and the number of correct responses was counted. The chance level then was 25%. This was decided due to the the premise that the participant was just instructed to point to the location of the building without explicit precision requirement. See Supplementary Table 11 for individual scores.

Emotional Memory. The score was calculated as the number of responses per run, which, under attentive participation, should equal the total number of trials. See Supplementary Table 12 for individual scores.

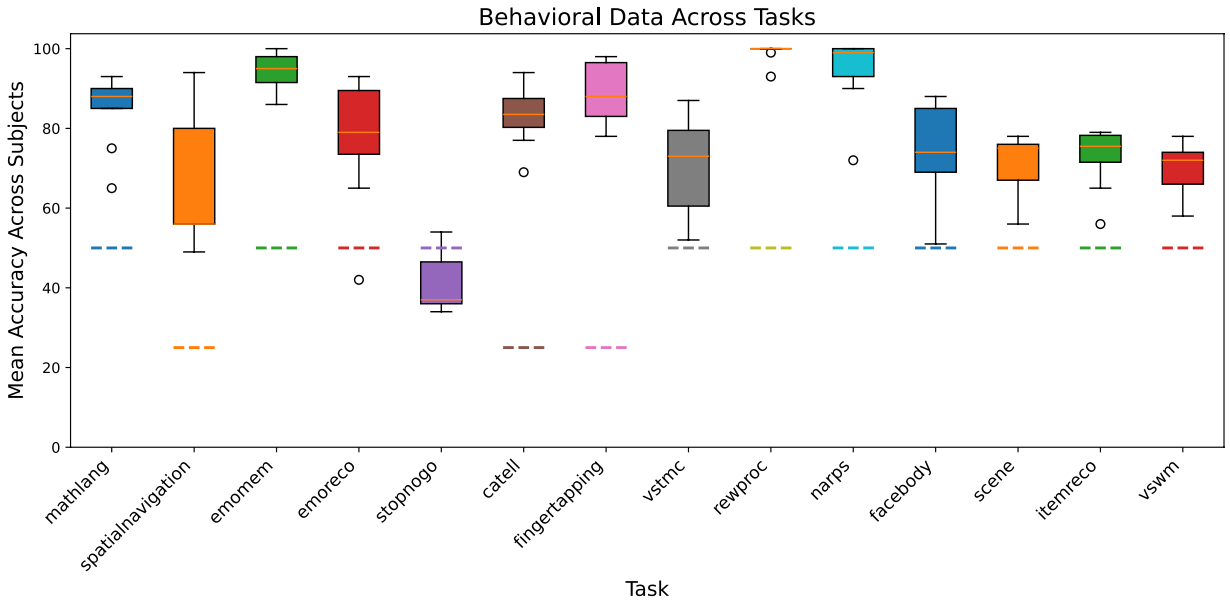

Fig. 5 Distribution of Individual Scores for Each Tasks.Boxplots summarizing the distribution of individual scores for each task featuring in this release. Orange lines indicate the mean score across subjects, while dotted lines represent the chance level for each task. Individual scores for each run, as well as averages across runs for every task, are provided in the supplementary material.

Emotion Recognition. Score was calculated as the number of correct responses, with a chance level of 50%. Missed responses were considered as incorrect. See Supplementary Table 13 for individual scores.

StopNoGo. The score was calculated as the number of trials in which they succeeded in withholding their response during Stop trials. The chance level was set at 50%. See Supplementary Table 14 for individual scores.

Catell (Oddball). The score was calculated as the number of correct responses, with a chance level of 25%. See Supplementary Table 15 for individual scores.

Finger Tapping. The score was calculated as the number of correct responses, meaning the number of times the subject pressed the correct button on specified trials plus the times they pressed a button within the selected fingers on chosen trials. The chance level was 25%. See Supplementary Table 16 for individual scores.

Visual Short Term Memory. Subjects could make 360 degrees rotations of the probe, and a response would be considered correct of the final angle would be within 45 absolute degrees of the correct direction. The score was calculated as the number of correct responses. See Supplementary Table 17 for individual scores.

Reward Processing. The score was calculated as the number of responses per run, which, under attentive participation, should equal the total number of trials. The chance level is set at 50%. See Supplementary Table 18 for individual scores.

NARPS. The score was calculated as the number of responses made during a run. The chance level is set at 50%. See Supplementary Table 19 for individual scores.

FaceBody. Score was calculated based on the number of correct responses. Missed responses were counted as incorrect. See Supplementary Table 20 for individual scores.

Scene. For each run, four scores were calculated: the number of possible scenes judged correctly, the number of impossible scenes judged correctly, the amount of possible scrambled dots correctly located, and the number of impossible scrambled dots correctly located. Missing responses were counted as incorrect, with a chance level of 50% for each one of the scores. See Supplementary Table 21 for individual scores.

Item Recognition. The score was calculated as the number of correct decisions. Missed responses were marked as incorrect, and the chance level was 50%. See Supplementary Table 22 for individual scores.

Visual search, working memory. The score was calculated as the sum of correct responses in both types of trials. Missing responses were marked as incorrect, and the chance level was 50%. See Supplementary Table 23 for individual scores.

Usage Notes

As mentioned earlier, the EBRAINS platform is the main repository for the data. Users can access and download the data through its graphical interface. To ensure GDPR compliance, access is granted upon creating an account with an institutional email address. Registration at EBRAINS is necessary due to the sensitive nature of neuroimaging data, which may potentially lead to the identification of individuals, even after de-identification procedures. By requiring institutional email addresses, EBRAINS helps to address privacy concerns.

Protocol Implementation Code. All scripts, routines and files we used for the protocols' acquisition are publicly available at the IBC repository: https://github.com/individual-brain-charting/public_protocols. Users are welcome to open issues for any questions or suggestions regarding the protocols. For each protocol, we have released the following files:

- *README:* a file containing a general description of the protocol with the main requirements and directions on how to reproduce each run.
- *Source code:* scripts and files for the execution of the protocol.
- *Stimuli:* files containing the stimuli used in the protocol.
- *Paradigm descriptors:* Python script to extract event-related files from the log files.
- *Instructions:* set of written instructions for the participants.

Data Analysis Code. Code to replicate the analyses featured in the figures of this paper can be accessed at: https://github.com/individual-brain-charting/public_analysis_code/. The scripts used for data analysis are available on GitHub under the Simplified BSD license.

Data Fetching Helper. We have developed a Python interface to facilitate data retrieval from the EBRAINS repository, to allow users to download the data with just a few lines of code. It is available at: https://github.com/individual-brain-charting/api.

Data availability

The IBC dataset is publicly available through the EBRAINS Knowledge Graph platform[71–74]. As of this release, the IBC project has incorporated 67 tasks, encompassing over 340 unique conditions and 530 independent contrasts, resulting in approximately 40 hours of fMRI data per participant. Data collection concluded in Fall 2023, with the final data release anticipated by the end of 2026. This forthcoming release aims to expand the dataset to 50 hours of fMRI data per participant, featuring 80 diverse tasks and over 700 independent contrasts. It will include new paradigms focusing on color perception, abstraction, tactile stimulation, and video gaming, among other cognitive domains.

Code availability

We have developed three main repositories: one for the protocols' routines, one for the data processing code, and one for a tool to access the data. Users are encouraged to open issues for any questions related to the code.

Received: 12 March 2025; Accepted: 9 February 2026;
Published online: 05 March 2026

References

1. Naselaris, T., Allen, E. & Kay, K. Extensive sampling for complete models of individual brains. *Current Opinion in Behavioral Sciences* **40**, 45–51, https://doi.org/10.1016/j.cobeha.2020.12.008 (2021).
2. Wang, M.-Y., Korbmacher, M., Eikeland, R. & Specht, K. Deep brain imaging of three participants across 1 year: The Bergen breakfast scanning club project. *Frontiers in Human Neuroscience*, **16**, https://doi.org/10.3389/fnhum.2022.1021503 (2022).
3. Elam, J. S. *et al*. The Human Connectome Project: A retrospective. *NeuroImage* **244**, 118543, https://doi.org/10.1016/j.neuroimage.2021.118543 (2021).
4. Varoquaux, G. *et al*. Atlases of cognition with large-scale brain mapping. *PLoS Computational Biology*, 14(11) https://doi.org/10.1371/journal.pcbi.1006565 (2018).
5. Gurevitch, J., Koricheva, J., Nakagawa, S. & Stewart, G. Meta-analysis and the science of research synthesis. *Nature* **555**, 175–182, https://doi.org/10.1038/nature25753 (2018).
6. Müller, V. I. *et al*. Ten simple rules for neuroimaging meta-analysis. *Neuroscience and Biobehavioral Reviews* **84**, 151–161, https://doi.org/10.1016/j.neubiorev.2017.11.012 (2018).
7. Poldrack, R. A. *et al*. Long-term neural and physiological phenotyping of a single human. *Nature Communications* **6**, 8885, https://doi.org/10.1038/ncomms9885 (2015).
8. Pinho, A. L. *et al*. Subject-specific segregation of functional territories based on deep phenotyping. *Human Brain Mapping* **42**, 841–870, https://doi.org/10.1002/hbm.25189 (2021).
9. Nee, D. E. fMRI replicability depends upon sufficient individual-level data. *Communications Biology* **2**, 1–4, https://doi.org/10.1038/s42003-018-0073-z (2019).
10. Michon, K. J., Khammash, D., Simmonite, M., Hamlin, A. M. & Polk, T. A. Person-specific and precision neuroimaging: Current methods and future directions. *NeuroImage* **263**, 119589, https://doi.org/10.1016/j.neuroimage.2022.119589 (2022).
11. Pinho, A. L. *et al*. Individual Brain Charting, a high-resolution fMRI dataset for cognitive mapping. *Scientific Data* **5**, 180105, https://doi.org/10.1038/sdata.2018.105 (2018).
12. Pinho, A. L. *et al*. Individual Brain Charting dataset extension, second release of high-resolution fMRI data for cognitive mapping. *Scientific Data*, 7(1). https://doi.org/10.1038/s41597-020-00670-4 (2020).
13. Pinel, P. *et al*. Fast reproducible identification and large-scale databasing of individual functional cognitive networks. *BMC Neuroscience* **8**, 91, https://doi.org/10.1186/1471-2202-8-91 (2007).
14. Barch, D. M. *et al*. Function in the human connectome: Task-fMRI and individual differences in behavior. *NeuroImage* **80**, 169–189, https://doi.org/10.1016/j.neuroimage.2013.05.033 (2013).

15. Humphries, C., Binder, J. R., Medler, D. A. & Liebenthal, E. Syntactic and semantic modulation of neural activity during auditory sentence comprehension. *Journal of Cognitive Neuroscience* **18**, 665–679, https://doi.org/10.1162/jocn.2006.18.4.665 (2006).
16. Binder, J. R. *et al*. Mapping anterior temporal lobe language areas with fMRI: A multicenter normative study. *NeuroImage* **54**, 1465–1475, https://doi.org/10.1016/j.neuroimage.2010.09.048 (2011).
17. Gauthier, B. & van Wassenhove, V. Cognitive mapping in mental time travel and mental space navigation. *Cognition* **154**, 55–68, https://doi.org/10.1016/j.cognition.2016.05.015 (2016).
18. Gauthier, B. & van Wassenhove, V. Time is not space: Core computations and domain-specific networks for mental travels. *Journal of Neuroscience* **36**, 11891–11903, https://doi.org/10.1523/JNEUROSCI.1400-16.2016 (2016).
19. Gauthier, B., Pestke, K. & van Wassenhove, V. Building the arrow of time……over time: A sequence of brain activity mapping imagined events in time and space. *Cerebral Cortex* **29**, 4398–4414, https://doi.org/10.1093/cercor/bhy320 (2018).
20. Lebreton, M., Abitbol, R., Daunizeau, J. & Pessiglione, M. Automatic integration of confidence in the brain valuation signal. *Nature Neuroscience* **18**, 1159–1167, https://doi.org/10.1038/nn.4064 (2015).
21. Dodell-Feder, D., Koster-Hale, J., Bedny, M. & Saxe, R. fMRI item analysis in a theory of mind task. *NeuroImage* **55**, 705–712, https://doi.org/10.1016/j.neuroimage.2010.12.040 (2011).
22. Jacoby, N., Bruneau, E., Koster-Hale, J. & Saxe, R. Localizing Pain Matrix and Theory of Mind networks with both verbal and non-verbal stimuli. *NeuroImage* **126**, 39–48, https://doi.org/10.1016/j.neuroimage.2015.11.025 (2016).
23. Genon, S. *et al*. Cognitive and neuroimaging evidence of impaired interaction between self and memory in Alzheimer's disease. *Cortex* **51**, 11–24, https://doi.org/10.1016/j.cortex.2013.06.009 (2014).
24. Pinho, A. L. *et al*. Individual Brain Charting third release, probing brain activity during movie watching and retinotopic mapping. *Scientific Data* **11**, 590, https://doi.org/10.1038/s41597-024-03390-1 (2024).
25. Nishimoto, S. *et al*. Reconstructing visual experiences from brain activity evoked by natural movies. *Current Biology* **21**, 1641–1646, https://doi.org/10.1016/j.cub.2011.08.031 (2011).
26. Sereno, M. I. *et al*. Borders of multiple visual areas in humans revealed by functional magnetic resonance imaging. *Science* **268**, 889–893, https://doi.org/10.1126/science.7754376 (1995).
27. Haxby, J. V. *et al*. A common, high-dimensional model of the representational space in human ventral temporal cortex. *Neuron* **72**, 404–416, https://doi.org/10.1016/j.neuron.2011.08.026 (2011).
28. Eisenberg, I. W. *et al*. Applying novel technologies and methods to inform the ontology of self-regulation. *Behav. Res. Ther* **101**, 46–57, https://doi.org/10.1016/j.brat.2017.09.014 (2017).
29. Santoro, R. *et al*. Reconstructing the spectrotemporal modulations of real-life sounds from fMRI response patterns. *Proc. Natl. Acad. Sci. USA* **114**, 4799–4804, https://doi.org/10.1073/pnas.1617622114 (2017).
30. Perrone-Bertolotti, M. *et al*. How silent is silent reading? Intracerebral evidence for top-down activation of temporal voice areas during reading. *J. Neurosci* **32**, 17554–17562, https://doi.org/10.1523/JNEUROSCI.2982-12.2012 (2012).
31. Vidal, J. R. *et al*. Category-specific visual responses: an intracranial study comparing gamma, beta, alpha, and ERP response selectivity. *Front. Hum. Neurosci* **4**, 195, https://doi.org/10.3389/fnhum.2010.00195 (2010).
32. Saignavongs, M. *et al*. Neural activity elicited by a cognitive task can be detected in single-trials with simultaneous intracerebral EEG-fMRI recordings. *Int. J. Neural Syst* **27**, 1750001, https://doi.org/10.1142/S0129065717500010 (2017).
33. Hamamé, C. M. *et al*. Reading the mind's eye: online detection of visuo-spatial working memory and visual imagery in the inferior temporal lobe. *Neuroimage* **59**, 872–879, https://doi.org/10.1016/j.neuroimage.2011.07.087 (2012).
34. Ossandón, T. *et al*. Efficient "pop-out" visual search elicits sustained broadband gamma activity in the dorsal attention network. *J. Neurosci* **32**, 3414–3421, https://doi.org/10.1523/JNEUROSCI.6048-11.2012 (2012).
35. Amalric, M. & Dehaene, S. Origins of the brain networks for advanced mathematics in expert mathematicians. *Proc. Natl. Acad. Sci. USA* **113**, 4909–4917, https://doi.org/10.1073/pnas.1603205113 (2016).
36. Diersch, N., Valdes-Herrera, J. P., Tempelmann, C. & Wolbers, T. Increased hippocampal excitability and altered learning dynamics mediate cognitive mapping deficits in human aging. *J. Neurosci* **41**, 3204–3221, https://doi.org/10.1523/JNEUROSCI.0528-20.2021 (2021).
37. Shafto, M. A. *et al*. The Cambridge Centre for Ageing and Neuroscience (Cam-CAN) study protocol: a cross-sectional, lifespan, multidisciplinary examination of healthy cognitive ageing. *BMC Neurol* **14**, 204, https://doi.org/10.1186/s12883-014-0204-1 (2014).
38. O'Doherty, J., Kringelbach, M. L., Rolls, E. T., Hornak, J. & Andrews, C. Abstract reward and punishment representations in the human orbitofrontal cortex. *Nat. Neurosci* **4**, 95–102, https://doi.org/10.1038/82959 (2001).
39. Botvinik-Nezer, R. *et al*. fMRI data of mixed gambles from the Neuroimaging Analysis Replication and Prediction Study. *Sci. Data* **6**, 106, https://doi.org/10.1038/s41597-019-0113-7 (2019).
40. Stigliani, A., Weiner, K. S. & Grill-Spector, K. Temporal processing capacity in high-level visual cortex is domain specific. *J. Neurosci* **35**, 12412–12424, https://doi.org/10.1523/JNEUROSCI.4822-14.2015 (2015).
41. Douglas, D. *et al*. Perception of Impossible Scenes Reveals Differential Hippocampal and Parahippocampal Place Area Contributions to Spatial Coherency. *Hippocampus* **27**, 61–76, https://doi.org/10.1002/hipo.22673 (2017).
42. Keator, D. B. *et al*. The Function Biomedical Informatics Research Network Data Repository. *NeuroImage* **124**, 1074–1079, https://doi.org/10.1016/j.neuroimage.2015.09.003 (2016).
43. Kuo, B.-C., Nobre, A. C., Scerif, G. & Astle, D. E. Top–Down activation of spatiotopic sensory codes in perceptual and working memory search. *J. Cogn. Neurosci* **28**, 996–1009, https://doi.org/10.1162/jocn_a_00952 (2016).
44. Poldrack, R. *et al*. The cognitive atlas: toward a knowledge foundation for cognitive neuroscience. *Front. Neuroinform* **5**, 17, https://doi.org/10.3389/fninf.2011.00017 (2011).
45. Gordon, E. M. *et al*. Precision functional mapping of individual human brains. *Neuron* **95**, 791–807.e7, https://doi.org/10.1016/j.neuron.2017.07.011 (2017).
46. Chang, N. *et al*. BOLD5000, a public fMRI dataset while viewing 5000 visual images. *Sci. Data* **6**, 49, https://doi.org/10.1038/s41597-019-0052-3 (2019).
47. Allen, E. J. *et al*. A massive 7T fMRI dataset to bridge cognitive neuroscience and artificial intelligence. *Nat. Neurosci* **25**, 116–126, https://doi.org/10.1038/s41593-021-00962-x (2022).
48. Bellec, P. & Boyle, J., *Bridging the gap between perception and action: the case for neuroimaging, AI and video games* https://doi.org/10.31234/osf.io/3epws (2019).
49. Gorgolewski, K. *et al*. The Brain Imaging Data Structure: a standard for organizing and describing outputs of neuroimaging experiments. *Sci. Data* **3**, 160044, https://doi.org/10.1038/sdata.2016.44 (2016).
50. Oldfield, R. C. The assessment and analysis of handedness: the Edinburgh inventory. *Neuropsychologia* **9**, 97–113, https://doi.org/10.1016/0028-3932(71)90067-4 (1971).
51. Chang, D. H. F., Ban, H., Ikegaya, Y., Fujita, I. & Troje, N. F. Cortical and subcortical responses to biological motion. *NeuroImage* **174**, 87–96, https://doi.org/10.1016/j.neuroimage.2018.03.013 (2018).
52. Johansson, G. Visual perception of biological motion and a model for its analysis. *Percept. Psychophys* **14**, 201–211, https://doi.org/10.3758/BF03212378 (1973).
53. Amalric, M. & Dehaene, S. A distinct cortical network for mathematical knowledge in the human brain. *NeuroImage* **189**, 19–31, https://doi.org/10.1016/j.neuroimage.2019.01.001 (2019).
54. O'Doherty, J., Critchley, H., Deichmann, R. & Dolan, R. J. Dissociating valence of outcome from behavioral control in human orbital and ventral prefrontal cortices. *J. Neurosci.* **23**, 7931–7939, https://doi.org/10.1523/JNEUROSCI.23-21-07931.2003 (2003).

55. Tom, S. M., Fox, C. R., Trepel, C. & Poldrack, R. A. The neural basis of loss aversion in decision-making under risk. *Science* **315**, 515–518, https://doi.org/10.1126/science.1134239 (2007).
56. Endo, N., Saiki, J., Nakao, Y. & Saito, H. Perceptual judgments of novel contour shapes and hierarchical descriptions of geometrical properties. *Japanese Journal of Psychology* https://doi.org/10.4992/jjpsy.74.346 (2003).
57. Moeller, S. *et al*. Multiband multislice GE-EPI at 7 Tesla, with 16-fold acceleration using partial parallel imaging with application to high spatial and temporal whole-brain fMRI. *Magn Reson Med* **63**, 1144–1153, https://doi.org/10.1002/mrm.22361 (2010).
58. Feinberg, D. A. *et al*. Multiplexed echo planar imaging for sub-second whole brain fMRI and fast diffusion imaging. *PLoS One* **5**, e15710, https://doi.org/10.1371/journal.pone.0015710 (2010).
59. Li, X., Morgan, P. S., Ashburner, J., Smith, J. & Rorden, C. The first step for neuroimaging data analysis: DICOM to NIfTI conversion, J. Neurosci. Methods volume264 https://doi.org/10.1016/j.jneumeth.2016.03.001 (2016).
60. Bischoff-Grethe, A. *et al*. A technique for the deidentification of structural brain MR images. *Hum Brain Mapp* **28**, 892–903, https://doi.org/10.1002/hbm.20312 (2007).
61. Smith, S. *et al*. Advances in functional and structural MR image analysis and implementation as FSL. *Neuroimage* **23**, S208–S219, https://doi.org/10.1016/j.neuroimage.2004.07.051 (2004).
62. Andersson, J. L. R., Skare, S. & Ashburner, J. How to correct susceptibility distortions in spin-echo echo-planar images: application to diffusion tensor imaging. *Neuroimage* **20**, 870–888, https://doi.org/10.1016/S1053-8119(03)00336-7 (2003).
63. Friston, K. J., Frith, C. D., Frackowiak, R. S. J. & Turner, R. Characterizing dynamic brain responses with fMRI: a multivariate approach. *Neuroimage* **2**, 166–172, https://doi.org/10.1006/nimg.1995.1019 (1995).
64. Ashburner, J. & Friston, K. Multimodal image coregistration and partitioning–a unified framework. *Neuroimage* **6**, 209–217, https://doi.org/10.1006/nimg.1997.0290 (1997).
65. Ashburner, J. & Friston, K. J. Unified segmentation. *Neuroimage* **26**, 839–851, https://doi.org/10.1016/j.neuroimage.2005.02.018 (2005).
66. Friston, K. J. *et al*. Event-Related fMRI: Characterizing Differential Responses. *Neuroimage* **7**, 30–40, https://doi.org/10.1006/nimg.1997.0306 (1998).
67. Friston, K. J., Josephs, O., Rees, G. & Turner, R. Nonlinear event-related responses in fMRI. *Magn Reson Med* **39**, 41–52, https://doi.org/10.1002/mrm.1910390109 (1998).
68. Abraham, A. *et al*. Machine learning for neuroimaging with scikit-learn. *Front Neuroinform* **8**, 14, https://doi.org/10.3389/fninf.2014.00014 (2014).
69. Amunts, K.*et al*. Linking Brain Structure, Activity, and Cognitive Function through Computation., *eNeuro***9**(2) https://doi.org/10.1523/ENEURO.0316-21.2022 (2022).
70. Wilkinson, M. D. *et al*. The Fair Guiding Principles for scientific data management and stewardship. *Scientific Data* **3**, 160018, https://doi.org/10.1038/sdata.2016.18 (2016).
71. Aggarwal, H., Ponce, A.F. & Thirion, B., Individual Brain Charting (IBC) (v4.0). EBRAINS https://doi.org/10.25493/S7GR-CT0 (2025).
72. Aggarwal, H., Ponce, A.F. & Thirion, B., Preprocessed data from the Individual Brain Charting (IBC) project (v2.0). EBRAINS https://doi.org/10.25493/4ZZ6-5S5 (2025).
73. Aggarwal, H., Ponce, A.F. & Thirion, B., 3mm-preprocessed data from the Individual Brain Charting (IBC) project (v2.1). EBRAINS https://doi.org/10.25493/DTEX-HWU (2025).
74. Aggarwal, H., Ponce, A.F. & Thirion, B., Contrast maps obtained from Individual Brain Charting (v3.0). EBRAINS https://doi.org/10.25493/873R-QK2 (2024).
75. Ponce, A.F., Supplementary tables for individual brain charting data descriptor (v5). figshare https://doi.org/10.6084/m9.figshare.30061798.v1 (2025).
76. Murphy, K., Bodurka, J. & Bandettini, P. A. How long to scan? The relationship between fMRI temporal signal to noise ratio and necessary scan duration. *Neuroimage* **34**, 565–574, https://doi.org/10.1016/j.neuroimage.2006.09.032 (2007).
77. Power, J. D., Barnes, K. A., Snyder, A. Z., Schlaggar, B. L. & Petersen, S. E. Spurious but systematic correlations in functional connectivity MRI networks arise from subject motion. *Neuroimage* **59**, 2142–2154, https://doi.org/10.1016/j.neuroimage.2011.10.018 (2012).
78. Lazar, N. A., Luna, B., Sweeney, J. A. & Eddy, W. F. Combining Brains: A Survey of Methods for Statistical Pooling of Information. *NeuroImage* **16**, 538–550, https://doi.org/10.1006/nimg.2002.1107 (2002).

Acknowledgements

We thank extensively the IBC project participants for their time and commitment to this long-term project, their disposition to perform many hours of MRI scanning over the years is what makes this project possible. We thank colleagues from the Cambridge Centre for Ageing and Neuroscience *CamCAN* for the availability of their protocols and their collaboration on having them reproduced in the IBC project. We thank colleagues from the Aging and Cognition Research Group at the German Center for Neurodegenerative Diseases (DZNE) for their collaboration on the implementation of the *Spatial Navigation* protocol. We thank colleagues from the Wellcome Centre for Human Neuroimaging at University College London for their collaboration on the integration of the *Reward Processing* protocol. We thank colleagues from the Schonberg Laboratory at Tel Aviv University for their support and collaboration on the implementation of the *NARPS* protocol on the IBC project. We thank colleagues from the Department of Psychology and the Stanford Neurosciences Institute at Stanford University for their collaboration on having the *FaceBody* protocol reproduced in the IBC project. We thank colleagues from the Department of Psychology at the University of Toronto for the collaboration on having the *Scene* protocol reproduced in the IBC project. We thank the Department of Psychiatry and Human Behavior at the University of California for their collaboration on the implementation of the *FBIRN battery* on the IBC project. We thank colleagues from the University of Rochester and the University of London for their collaboration on having the *Visual Search* protocol reproduced in the IBC project. We thank the Center for Magnetic Resonance Research, University of Minnesota for having kindly provided the Multi-Band Accelerated EPI Pulse Sequence and Reconstruction Algorithms. This project has received funding from the European Union's Horizon 2020 Framework Program for Research and Innovation under Grant Agreement No 720270 (Human Brain Project SGA1) and 785907 (Human Brain Project SGA2). Ana Luísa Pinho is the recipient of a BrainsCAN Postdoctoral Fellowship at Western University, funded by the Canada First Research Excellence Fund (CFREF).

Author contributions

A.F.P. performed MRI acquisitions, produced task annotations, contributed to the development of tools for the dataset, wrote the documentation and wrote this manuscript. H.A. performed MRI acquisitions, set task protocols, produced annotations, wrote the documentation, developed tools for the dataset and designed

some analyses. S.S. performed MRI acquisitions, set task protocols, produced annotations and wrote the documentation. J.J.T. performed MRI acquisitions, set task protocols, produced annotations and wrote the documentation. A.L.P. performed MRI acquisitions, set task protocols, produced annotations, wrote the documentation and took part in the general design of the study. A.T. contributed to the design of the study, the development of tools and data analyses. C.G., Y.L., V.B., and L.B. performed the MRI acquisitions plus visual inspection of the neuroimaging data for quality-checking. L.L., V.J.-T. and G.M.-C. recruited the participants and managed routines related to appointment scheduling and ongoing medical assessment. L.H.-P. conceived the general design of the study and wrote the ethical protocols. C.D. recruited the participants and managed the scientific communication of the project with them. B.M. managed regulatory issues. M.A. and S.D. conceived the general design of the study and made the MathLanguage protocol integration into IBC possible. N.D. and T.W. assisted with the integration of the SpatialNavigation protocol. M.A.S. supervised integration of the CamCAN battery: EmoMem, EmoReco, StopNogo, Catell, FingerTapping and VSTMC protocols. J.P.OD., V.M. and R.J.D. supervised integration of the Reward Processing protocol. R.A.P. supervised implementation of the gambling protocols, later incorporated into the NARPS protocol. A.S. and K.G.S. supervised integration of the FaceBody protocol. D.D. and A.C.H.L supervised integration of the Scene protocol. D.B.K. and S.G.P. supervised integration of the FBIRN battery: ItemRecognition, BreathHolding, Checkerboard and FingerTap protocols. D.H.F. and N.F.T. made the BiologicalMotion protocol integration into IBC possible. B.-C.K. and D.E.A. made the VisualSearch protocol integration into IBC possible. B.T. conceived the general design of the study, managed the project, wrote the ethical protocols, pre-processed fMRI data, performed the analysis of the fMRI data, developed FastSRM, developed Nilearn, developed Pypreprocess, developed the IBC public analysis pipeline, uploaded IBC collections on EBRAINS and contributed to the IBC documentation.

Competing interests

The authors declare no competing interests.

Additional information

Correspondence and requests for materials should be addressed to A.F.P.

Reprints and permissions information is available at www.nature.com/reprints.

Publisher's note Springer Nature remains neutral with regard to jurisdictional claims in published maps and institutional affiliations.